Study of nuclear recoils in liquid argon with monoenergetic neutrons

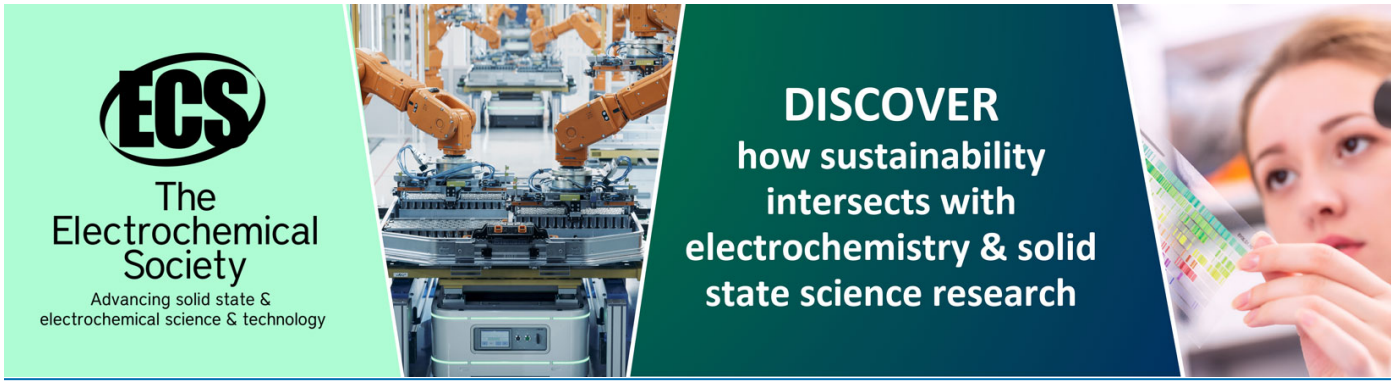

12th International Conference on Topics in Astroparticle and Underground Physics (TAUP 2011) IOP Publishing
Journal of Physics: Conference Series **375** (2012) 012019 doi:10.1088/1742-6596/375/1/012019

Study of nuclear recoils in liquid argon with monoenergetic neutrons

C. Regenfus, Y. Allkofer, C. Amsler, W. Creus, A. Ferella, J. Rochet, M. Walter

Physik-Institut der Universität Zürich, CH–8057 Zürich, Switzerland

E-mail: regenfus@cern.ch

Abstract. In the framework of developments for liquid argon dark matter detectors we assembled a laboratory setup to scatter neutrons on a small liquid argon target. The neutrons are produced mono-energetically (E_{kin}=2.45 MeV) by nuclear fusion in a deuterium plasma and are collimated onto a 3" liquid argon cell operating in single-phase mode (zero electric field). Organic liquid scintillators are used to tag scattered neutrons and to provide a time-of-flight measurement. The setup is designed to study light pulse shapes and scintillation yields from nuclear and electronic recoils as well as from alpha particles at working points relevant for dark matter searches. Liquid argon offers the possibility to scrutinise scintillation yields in noble liquids with respect to the population strength of the two fundamental excimer states. Here we present experimental methods and first results from recent data towards such studies.

1. Introduction

Over the last years liquid xenon TPCs [1, 2] established themselves among the leading technologies for WIMP searches. Furthermore considerable effort is being made by various groups to bring the liquid argon (LAr) sector to a competitive level in this respect [3]. Liquid argon has the potential to be a large and sensitive multi purpose detector due to its low ionisation potential and large abundance on earth. Interest in the low energy frontier of this technology increased by recent progress in the production of ^{39}Ar depleted argon from dwell gases. Here we describe research activities which are part of the design study for a next generation dark matter facility, DARWIN [4], presently proposed as a combined liquid xenon - liquid argon installation.

WIMPs, hypothesised to be distributed as a thermalised halo in our galaxy, should produce nuclear recoils in any target on earth, which can be detected and isolated in noble liquids through their characteristic excitation and ionisation patterns. However the complex microscopic processes which lead eventually to the scintillation and charge signals are not very well understood at low energies and are currently the subject of large experimental controversy. The experimental determination of light and charge yields at keV energies and possibly below is therefore of highest interest for this research since it defines the energy scale and sensitivity of the experiment. The uncertainty in the signal calibration of nuclear recoils still yields the largest contribution to the systematical error for liquid xenon WIMP searches [1, 5] despite the large efforts of various groups [5, 6] to determine this quantity. In the liquid argon sector the situation is even worse, only scarce information about the scintillation efficiency can be found in literature [7, 8] and no comprehensive measurement of the charge yield exists at all.

The energy dependent light yield Y_{nr} of nuclear recoils is commonly described by the unitless quantity $\mathcal{L}_{eff}$, the relative scintillation efficiency, determined in relation to the yield of recoiling electrons (Y_{er}) of same kinetic energy. By convention $\mathcal{L}_{eff}$ is measured at zero electric field. The

value of $\mathcal{L}_{\rm eff}$ is expected to decrease towards low energies, mainly due to the increasing fraction of nuclear stopping power, transferring energy to heat, described by Lindhard's theory [9, 10]. Additional (luminescence) quenching, which is less well understood, arises at high ionisation densities by interactions among the excited and ionised states created in the process of energy loss to electrons (electronic stopping). The light yield of recoiling electrons is not affected by nuclear effects and shows a linear response for energies above some tens of keV [11]. This allows for the convenient comparison of the energy scales of both recoil types, where $E_{\rm ee}$ represents the (equivalent) energy of an electron to produce the same amount of light as a recoiling nucleus with Energy $E_{\rm r}$. Electron yields are traditionally determined at the 122 keV line of ^{57}Co. Electric fields reduce the recombination of free charge carriers and decrease scintillation light [12]. In the estimation of light yields this effect is taken into account by two energy and field dependent correction functions $S_{\rm n}$ and $S_{\rm e}$, for nuclear and electronic recoils, respectively, which are unknown for liquid argon. In liquid xenon [13, 14] values for $S_{\rm n}$ are close to unity while $S_{\rm e}$ drops to below 0.5 at fields >1 kV/cm. This is due to screening effects at the large ionisation densities of nuclear recoils. Thus the relative scintillation efficiency can be calculated by $\mathcal{L}_{\rm eff} = Y_{\rm nr}/Y_{\rm er} \cdot S_{\rm e}/S_{\rm n} = E_{\rm ee}/E_{\rm r} \cdot S_{\rm e}/S_{\rm n}$. In this work the values for $S_{\rm e}$ and $S_{\rm n}$ are set to unity.

Liquid argon allows for a separate study of fast and slow components in the scintillation signal due to the large difference in their lifetimes. The analysis of pulse shapes [15] is an important tool for background discrimination in LAr dark matter detectors. Here we apply pulse shape analysis to light yield studies in regions of both, low and high ionisation densities in a noble liquid. In the following we present a brief overview of the experimental method and show first results obtained from data recorded under neutron, alpha and gamma irradiation in liquid argon at zero electric field.

2. Experimental Setup

We induce nuclear recoils in the liquid argon cell by fast neutrons (2.45 MeV) from a deuterium-fusion-generator made by the company NSD-Fusion, Germany. It delivers up to $2{\cdot}10^6$ isotropically emitted mono-energetic neutrons from the two-body reaction $\mathrm{dd} \rightarrow {}^3\mathrm{He} + \mathrm{n}$ ($\mathrm{dd} \rightarrow \mathrm{t} + \mathrm{p}$ is equally probable). The overall setup was developed in collaboration with the producer. The fusion rate in the deuterium plasma is controlled by an electrical DC field generated by an adjustable constant current (1-15 mA) HV supply. The voltage to keep the plasma current stable (30-120 kV) is regulated indirectly by the pressure of the deuterium gas which is released from heated getter disks storing deuterium on their surfaces. Higher voltage (lower gas pressure) produces higher fusion rates but also a harder bremsstrahlungs background spectrum. The environment is shielded from neutron and X-ray radiation by means of a 1600 kg polyester cylinder with 2 mm Pb cladding (fig. 1) keeping the radiation dose far below the limit of 2.5μSv/h imposed by CERN's radiation protection requirements. A safety area with access control and radiation interlock complete the setup. A polyethylene

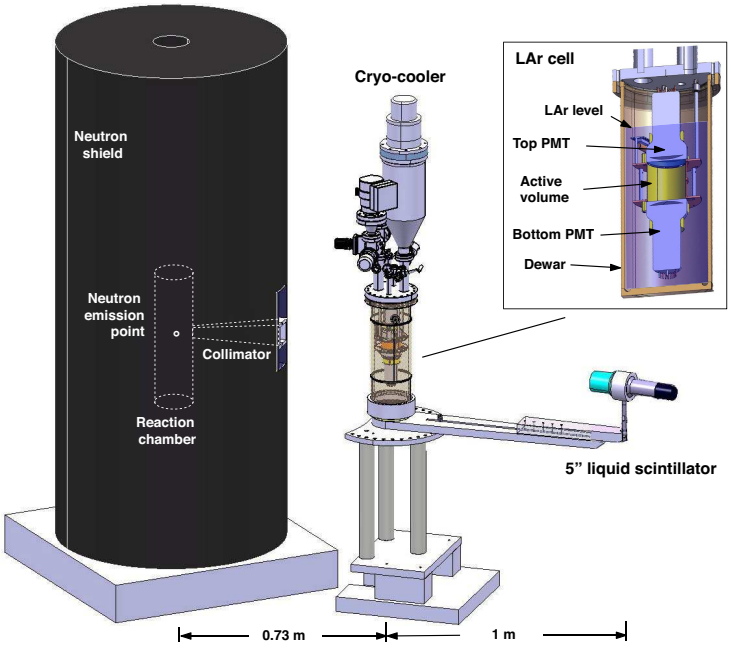

Figure 1. Setup of the scattering experiment with neutron generator, shield and zoom on the LAr cell.

collimator with square cross section allows for the emission of neutrons in a fixed solid angle of about 0.2% of 4π, covering fully the sensitive volume of the cryogenic LAr cell. For the measurements described here the cell was located at a distance of about 73 cm from the neutron emission point while the liquid scintillator counter (LSC) could be set at various scattering angles on a 1 m long arm rotatable around the centre of the cell. The nominal scattering angle is given from the two axes of neutron emission point to the centre of the LAr cell and further on to the centre of the liquid scintillator. Errors on angles or mechanical alignments were estimated to be below 0.5 degree. The internal structure of the cryogenic cell is shown in the inset of fig. 1. Two TPB coated 3" PMTs (Hamamatsu R6237-MOD) with bialkali photo cathodes and Pt underlay (QE≈15%) are arranged face to face at a distance of about 47 mm forming a cylindrical sensitive volume of roughly 0.2ℓ. This volume is defined by a thin Al cylinder holding the TPB coated reflector foil [1] to wave shift the VUV scintillation light. A small ^{210}Po alpha source of about 40 Bq activity is installed in the centre of the cell. The source was coated with some tens of μm plastic (Paraloid B-72) to spread the energies of emitted alphas over a broad range. The Al cylinder is polarised to the same voltage as the photo cathodes of the PMTs to keep the internal electrical field close to zero. A 60 ℓ/s turbo pump is used to evacuate the chamber to typically 10^{-6} mbar prior to filling with argon gas class 60 (impurities ≤ 1.3 ppm). A membrane pump provides for continuous recirculation via two in parallel mounted OXISORB-W cartridges which reduce the O_2 and H_2O levels to <5 and <30 ppb respectively. The gas is condensed on top of the chamber at the cold head of a Sumitomo CH210 cryocooler system with about 80 W cooling power driven by a Sumitomo F-70CH helium compressor. A LabView based slow control system regulates the cold head temperature and records temperatures, pressures and liquid levels. The analogue signals from the two PMTs are each split into 2 inputs of a LeCroy WavePro 35Zi DSO, sampled with 5000 points at 1 GS/s and stored to the hard drive. The splitting of the signals permits a large dynamic range to fully reconstruct alpha particles while maintaining high signal over noise ratios for single photons. Cosmic signals however can saturate the FADC [3]. Event triggers of coincidences and delays between PMT signals and external detectors were produced by means of the programable trigger logic in the oscilloscope. Signals of neutrons in the LSC are processed in a dedicated analogue pulse shape discriminator (Mesytec MPD4 [18]) and fed into the external input of the oscilloscope.

3. Data reconstruction and light yield

Scintillation signals in liquid argon are determined by numerical integration of the digitised photo currents of the two PMTs, normalised to their mean single photon charges. Due to the long integration times in LAr an iterative method was developed to calculate precise pedestal values on an event by event base. The sum of both channels yields the raw integrated pulse height (*IPH*) in units of photo electrons (pe). This value is furthermore corrected for the finite integration time, losses by software thresholds (clusterfinder) and most importantly by losses due to impurities in the liquid argon (see next chapter). Light yield calibrations were performed periodically during data taking by means of a strong external ^{241}Am source producing a prominent 60 keV photo peak in the integrated pulse height spectrum of the data (fig. 2 left). The gains of the PMTs were determined

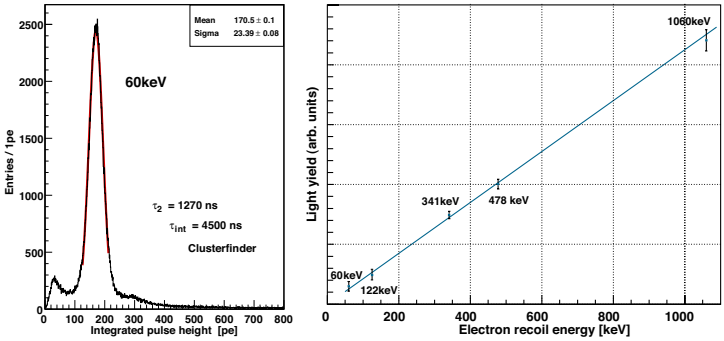

Figure 2. *Left: 60 keV line from the raw signals of the ^{241}Am data. Right: light yield of various photon sources.*

[1] 1 mg/cm^2 tetra-phenyl-butadiene (TPB) on Tetratex; PMT coatings 0.08 mg/cm^2 TPB. See [16, 17] for details

from LED pulses or single photon signals collected from event tails in the data. Single photon distributions are analysed for most probable values and corrected for asymmetry (+14.5%) to find the mean single photon charge. The gains during several weeks of data taking in summer 2011 were found to be stable within 2.7%. An average light yield of 3.75 ± 0.1 pe/keV has been determined over the whole run time. To check the linearity of the system we employed various external photon sources, ^{57}Co (122 keV photo peak), ^{22}Na (511 and 1275 keV Compton edges), as well as ^{137}Cs (662 keV Compton edge). Figure 2 (right) shows a linear fit to the raw measurements of these data which were taken under similar conditions.

4. Impurity effects – correction of light yields

In liquid argon VUV fluorescence from the so-called second continuum is the dominant mechanism for light emission under excitation. The light pulse shape is well described by the sum of two exponentials originating in the radiative decays of two fundamental excimer states. Atomic selection rules are the cause for a large difference in their lifetimes, τ_1 and τ_2, approximately 6 and 1600 ns, for singlet and triplet states, respectively. This feature is used for background discrimination in LAr dark matter detectors thanks to the ionisation density effect [15] modifying the pulse shape according to specific energy losses of particles. Suppression factors up to 3 orders of magnitude are reached [22] for recoil energies above 30keV$_r$ using a likelihood based discrimination method. The improvement of such algorithms is also part of our research but will be described elsewhere.

In the following we decompose individual or averaged signal traces by means of the sum of two exponential decays convoluted with a gaussian which describes general time spreads (2.9 ns). We denote the integrals of fast and slow scintillation components, representing the occurrences of singlet and triplet states, with A and B, respectively; A+B being the total measured light yield Y. Furthermore we denote the fraction $A/(A+B)$ as the component ratio CR, representing the relative strength of the fast portion of the scintillation light. We want to stress that values for CR are similar but somewhat different from the common variable for the prompt light fraction f_p, determined from short and long signal integrations.

Due to their long lifetime triplet states undergo various collisions with neighbours before they eventually decay. Thereby interactions with impurities can cause the (non-radiative) destruction of these states and hence induce losses in the scintillation light (impurity quenching [20, 21]). This process occurs in competition to the natural decay of the states and results in an apparent reduction of the triplet lifetime τ_2 in the data [2]. On account of the normalisation of the exponential PDF the corrected light yield [20] is found from the relation

$$Y_{\mathrm{cor}} = A + B_{\mathrm{cor}} = A + B/\tau_2 \cdot \tau_2^{\max} ,$$

where B_{cor} is the extrapolated yield of the triplet component and $\tau_2^{\max}$ the undisturbed lifetime of triplet states in LAr (1600 ns [15, 19]). The fraction B/τ_2, corresponding to the triplet decay rate at t=0, is effectively invariant versus variations of purity and completely determined by the fit. In the same way the value for the corrected component ratio is given by $CR_{\mathrm{cor}} = A/(A+B_{\mathrm{cor}})$. Corrected light yields are conveniently calculated by $Y_{\mathrm{cor}} = A/CR_{\mathrm{cor}}$. As an example fig. 3 shows the two components of such fits to averaged signal traces of 60 keV calibration data versus the value found for τ_2 under

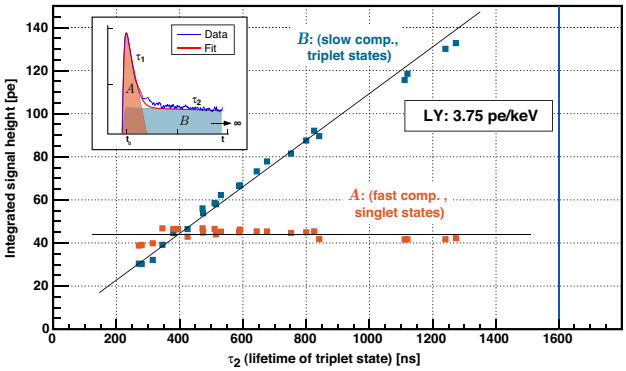

Figure 3. *Yield of the fast and slow scintillation components under different purity conditions.*

[2] In LAr the value for τ_2 can be used to estimate purity levels in respect to scintillation yields [19]. In this work purity levels are predetermined by residual H_2O on internal surfaces of the vacuum and gas system

different purity condition. Values for A remain unaffected (for purity conditions of $\tau_2 > 400\,\mathrm{ns}$) while B increases proportional to the measured τ_2. From these results we conclude that other quenching mechanisms, like VUV absorption by impurities, are not affecting light yields under the present geometrical conditions and purity levels. All yields as well as component ratios presented in the following are corrected for losses by impurities by the method presented here.

5. Time structure of the scintillation light

The well fitting exponential decay model assumes production and modification of excimer states being completed on time scales shorter than the measured decay constants. Moreover the experimentally observed invariance of lifetimes, i.e. their independence on ionisation densities, rules out [23] the participation of these states in the fast processes of luminescence quenching during production [3]. However, in the temporal transition region between fast and slowly decay modes, two component fits systematically underestimate the data. This situation can be improved by the introduction of a third component in the fit function. The relative contribution of such an extension scales with the value for CR and ranges between 3 and 7% of the total integral [24], lifetimes vary between 50 and 200 ns. The nature of this effect is presently not understood, possible explanations comprise PMT-after-glow and recombination light. In the context of this work we exclude the transition region from the fit, until the results of a systematic study on this effect, e.g. by measuring the electric field dependence of light pulse shapes.

In the following we compile measurements of component ratios determined from event-wise likelihood fits for recoiling Ar nuclei, alpha particles and electrons. The former were induced by 2.45 MeV neutrons from the generator, the second were emitted from the built-in ^{210}Po source, and the latter were induced by 511 keV photons from an external ^{22}Na source, respectively. As already mentioned the ^{210}Po source was coated with a thin layer of plastic to degrade and spread the energy of emitted alphas. Data for neutrons and alphas was purely triggered on signals in the liquid argon, while an additional coincidence with an external detector was required for the photon data to tag the emission of two 511 keV photons. This data was also used to determine the time calibration for the time-of-flight (TOF) measurement for scattered neutrons as well as the trigger roll off at small signal sizes. The latter is derived from the lower end of the Compton spectrum. While photon and alpha data are practically background free, nuclear

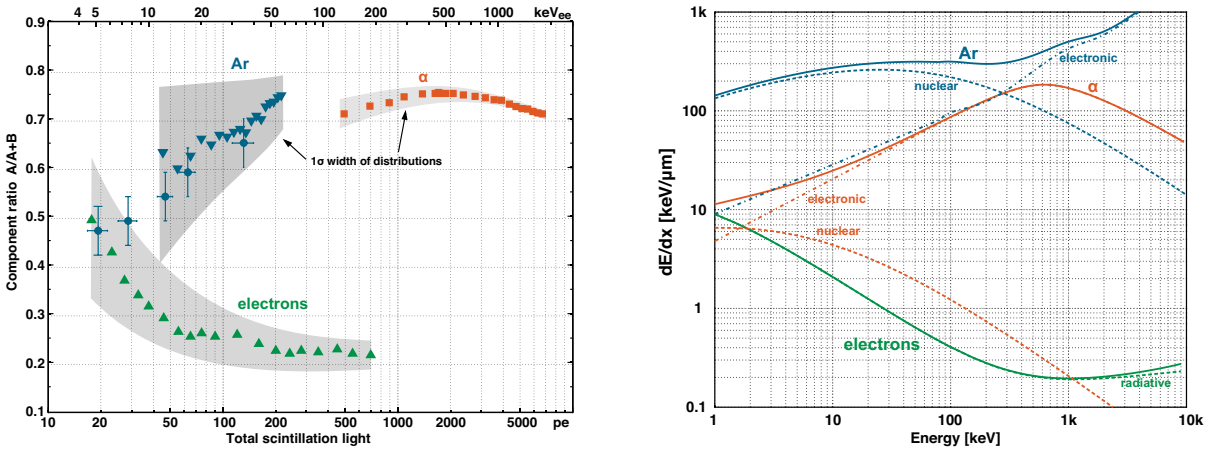

Figure 4. *Left: component ratio vs. signal size for argon, alpha and electron recoils. The grey zones illustrate the spread. Right: total stopping power (solid lines) and contributions (dashed lines).*

recoils suffer from a contamination with inelastic collisions from neutrons with argon nuclei producing photons. Due to the small geometric dimensions and the low kinetic energies however these events are estimated not to contribute more than 7% to this data. A Monte Carlo study

[3] Contrariwise quenching by impurities is a relatively slow process of destruction of (long lived) excimer states

is in progress. The software framework was tested for unbiased reconstruction of pulse shapes in respect to small signal heights. Therefor fixed-ratio test pulses were generated in the energy range of interest and analysed for flatness of *CR*. No significant deviation of the flat response could be found. Figure 4 to the left shows the component ratio versus the total amount of scintillation light produced by these particles. The two prominent bands from electrons (upward triangles) and nuclear recoils (downward triangles)merge for energies below about 10keV$_{\mathrm{ee}}$. Grey zones behind the data points illustrate the 1σ widths of the distributions, derived from gaussian fits of vertical slices. Errors are dominated by systematics introduced by the analysis method and are estimated to be roughly 0.25 of the distribution widths. The values at low energies for argon recoils are also shown (circles) and derived from fits to mean traces (see chap. 7). The right plot summarises the values of total stopping power for the same particles as well as the nuclear and electronic contributions. This data was collected from the websites of SRIM, ASTAR and ESTAR [25], respectively.

The correlation among both plots is easily observed, larger ionisation densities generally lead to larger fraction of singlet states in the scintillation light. This trend is also true for the regions towards smaller kinetic energies as well as for the maximum in the curves for alpha particles. Interesting is also the apparent value close to 0.25 for lowest ionisation densities, corresponding to a uncorrelated production of triplet and singlet states. According to their statistical weights just a factor of 3:1 is expected for the relative ratio in their populations. If (luminescence) quenching effects are neglected, deviations from the minimal value of 0.25 imply either the enhanced production of singlet states on the exciton level or the transfer from triplet to singlet states shortly after their production in the area of high ionisation density. Quenching effects among excimer states are excluded for the upper mentioned arguments of lifetime invariance. The physical relation between the specific production of excimer states and the prevailing specific energy deposit can be unfolded from these data if the integrated nature of the measurement is taken into account. In the next chapter we apply this method to alpha particles by using a simple linear relation for the relation between component ratio and linear energy transfer.

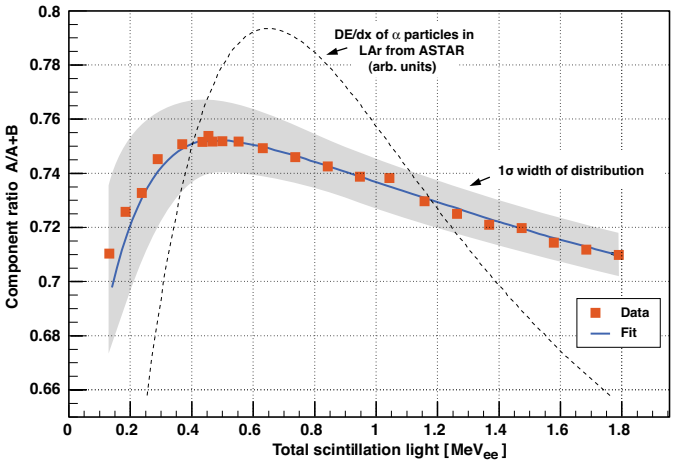

Figure 5. *Component ratio of alpha particles in LAr and fit vs. total scintillation light in units of* MeV$_{\mathrm{ee}}$.

6. Scintillation yield of alpha particles in LAr

In this section we extract the value for the relative scintillation yield $\mathcal{L}_{\mathrm{eff}}^{\alpha}$ of alpha particles by comparison of the shapes of the component ratio to linear energy transfer (*LET*). In good approximation the latter is assumed to be identical to the electronic stopping power $\mathrm{d}E/\mathrm{d}x\,(E)$. For the fit function we use a 10^{th} degree polynomial parametrisation of the ASTAR curve from fig. 4. The integrated nature is taken into account in a linear relation to the $\mathrm{d}E/\mathrm{d}x$ curve by the following relation,

$$CR(E) = \int_0^{x_{E=0}} \frac{\mathrm{d}CR(E)}{\mathrm{d}E} \cdot \mathrm{d}E/\mathrm{d}x\,(E)\,\mathrm{d}x \quad \text{with} \quad \frac{\mathrm{d}CR(E)}{\mathrm{d}E} = p_1 \cdot \mathrm{d}E/\mathrm{d}x\,(p_2 \cdot E) + p_3,$$

where E is energy, x the path of the alpha particle and p_i, $i = 1..3$ are the three free fit parameter defining the convolution of *LET* and *CR*. While p_3 describes an empiric vertical offset, p_2 is the parameter of interest introducing a scale for the energy dependent yield (quenching). The naive comparison of the maxima of both curves already gives a first estimate on the value for $\mathcal{L}_{\mathrm{eff}}^{\alpha}$,

being roughly 0.75 . Fig.5 shows the measurements for CR obtained by event-wise likelihood fits of the signal shape from alpha particles. The 1σ spread is again illustrated by the grey band. In general the fit (solid line) describes the data well but starts to deviate in the area of low energies probably due to our simple linear model. Also shown is the curve of the electronic stopping power for alpha particles in LAr from ASTAR (dotted line), which actually deviates less than 2% from the total stopping over this energy range. A value of 0.74±0.04 is found for the parameter p_2 from the fit. This corresponds to an estimate for the mean relative scintillation efficiency for alpha particles in LAr in a range of 0.18-2.5 MeV_r. The result agrees within the errors with the value of q_e=0.71 given in [11] for 5 MeV alpha particles assuming a nuclear quenching of $q_n = 0.98$. A similar value was also obtained in [23]. Due to their relatively small mass alpha particles in this energy range are only little affected by effects of nuclear quenching. The light loss of roughly 25% is hence entirely due to luminescence quenching effects.

7. Light yield of nuclear recoils in LAr

In this section we present the data taken in the experimental arrangement of the neutron generator described in chap. 2 . A 5" liquid scintillator (LSC) was used for triggering positioned under the nominal angles of 30, 40, 50, 60 and 90 degrees corresponding to 16.4, 28.5, 43.4, 60.5 and 120 keV recoil energies, respectively. Due to the geometrical extensions of the detectors scattering angles are distributed around the nominal angles roughly box-like (FWHM≈10.8 deg). In most cases the neutron generator was operated at 80 kV and 10 mA corresponding to the emission of about $2{\cdot}10^5$ neutrons per second in 4π. The settings were chosen mainly to compromise about background induced by bremsstrahlung (accidental coincidences). Under these settings about 1 neutron per minute scatters off an argon nucleus in the active volume and is detected in the liquid scintillator 1 m downstream. The direct line of sight between the exit of the collimator and the LSC was obstructed with a 20 cm thick sheet of polyethylene. Background rates amount roughly to 5 per minute originating mainly from two sources; firstly cosmic muons saturating the LSC output and faking a neutron signal in the analog pulse shape discriminator and secondly accidental coincidences between diffusively scattered neutrons and bremsstrahlung.

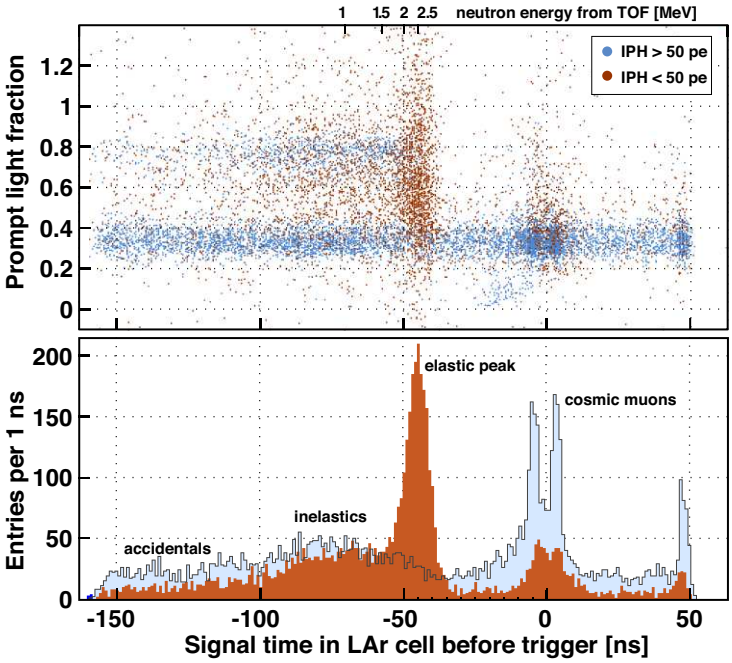

Figure 6. f_p *vs. signal time in LAr with projection on the x-axis, if a neutron triggered the liquid scintillator counter.*

A trigger is generated if in a window of -150...+50 ns around the arrival time of a neutron in the LSC an event was recorded by the liquid argon cell. Such an event is defined as both PMTs showing signals above 0.2 photoelectron pulse height in a 50 ns time coincidence. As an example fig. 6 shows the 19k events from the 30 deg scattering data. The upper plot displays the prompt light fraction of raw signals versus the time difference between the signal in the LAr cell and the arrival time of a neutron in the LSC (TOF). Events above 50 pe of IPH are printed in blue while events below are printed in brown. The histogram on the bottom shows the projection to the x-axis of the same events. The small signal distribution (brown) is dominated by elastically

scattered neutrons around the nominal flight time at roughly -45 ns. Also visible is a broad distribution of inelastic scatters where neutrons loose a substantial fraction of their energies. A small uniform background originates presumably in accidental coincidences of bremsstrahlung photons in the outer LAr volume. Two principle cuts are applied to select events. Firstly a time cut of a 5 ns window to the right of the most probable value of the elastic scatter peak and secondly the (loose) limit on *IPH* (typ. 50 pe). The latter removes very efficiently accidental coincidences with photons, inelastic scatters with large energy deposit in the LAr as well as cosmic muons. In the case of the 30 deg data we end up with roughly 1k events, shown in fig. 7. From these distributions we determine the value for A and CR, the former from the distribution mean and the latter by a fit to the mean trace of selected events. A more precise study by comparing the measured distributions to the ones generated by MC is in progress. We estimate roughly 15% background in the selected data (incl. double scatters). From a preliminary analysis of the 5 scattering angles we determine light yields as well as component ratios with errors of typically 15%. The errors are estimated from the reconstruction of A and CR and calculated according to the standard propagation law. Figure 8 to the left shows our measurements in comparison to [8] and the one averaged value

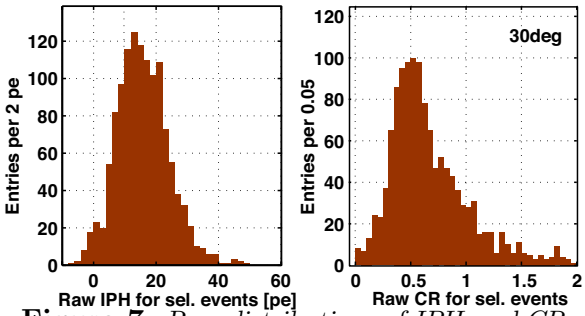

Figure 7. *Raw distributions of IPH and CR after the time and IPH cut.*

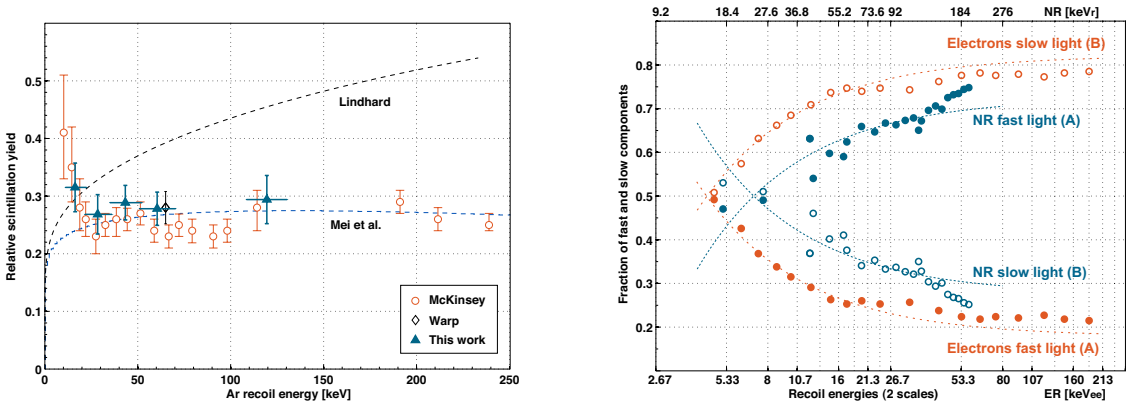

Figure 8. *Left: values for $\mathcal{L}_{\rm eff}$ with a comparison to theoretical curves and other published data. Right: relative scintillation components for nuclear recoils and electrons plotted against the two energy scales.*

from [7]. The measurements still allow for a flat interpretation of $\mathcal{L}_{\rm eff}$, leading to a mean value of $<\mathcal{L}_{\rm eff}> = 0.29 \pm 0.03$ for nuclear recoils at energies above 20keV$_{\rm r}$ or 6keV$_{\rm ee}$. At the present state of the analysis we can neither exclude nor confirm the increase of $\mathcal{L}_{\rm eff}$ at the low energy edge of the data from [8]. However we plan to upgrade the LAr cell with higher QE PMTs as well as to improve significantly on the argon cleaning system.

LAr features the possibility of a separate study of singlet and triplet contributions under quenching effects. This is shown by the relative values of A and B in fig. 8 (right), for nuclear recoils and electrons, respectively. The two energy scales are added to top and bottom. The dashed lines correspond to linear fits of the absolute values of A and B and are meant to guide the eye. A comparison with the theoretical description of luminescence quenching in LAr by a simple saturation law combined with the Lindhard model [11] favours the assumption of a constant value for $\mathcal{L}_{\rm eff}$. Hence these measurements are compatible with an interpretation of collisional spin change of triplet state excimers or a preferred production of singlet states excimers under higher ionisation densities during the selftrapping process of the excitons.

Summary and conclusions

We confirmed scintillation light quenching in liquid argon by impurities being of the same physical nature as observed in gaseous argon. In analogy to this we use measured lifetimes and component ratios to reconstruct purity independent results. Pulse shape analysis under different particle impacts, ionisation densities and correlated quenching effects can deliver new insight into quenching effects. We presented preliminary results from data taken in liquid argon under excitation with mono-energetic neutrons, alpha particles and photons at zero electric field. We confirm values for *CR* monotonically rising with values for *LET*. Moreover changes of *CR* seem to be decoupled from quenching processes and happen in regions with constant specific light yield. A component ratio close to the one expected from statistically populated singlet and triplet states (1/(1+3)=0.25) is observed for recoiling electrons in the region of lowest ionisation densities (uncorrelated production). For nuclear recoils we find the component ratio rising from values around 50% to 75% in an energy range from 20 to 200 keV. For alpha particles in the MeV range we determine a relative scintillation yield $\mathcal{L}_{\rm eff}^{\alpha}$ of 0.74±0.04 (luminescence quenching) and observe a slightly smaller *CR* as for recoiling nuclei. A preliminary analysis of the relative scintillation yield $\mathcal{L}_{\rm eff}$ for nuclear recoils at energies between 16 and 120 keV shows a flat response within present errors. A mean value $<\mathcal{L}_{\rm eff}> = 0.29\pm0.03$ was found. No conclusive results for energies below that region can be drawn at the present state of the analysis. In the near future we plan to upgrade the cell with PMTs of larger quantum efficiencies and to improve the cleaning system. At a later stage we plan to add an internal electric field and to extract the ionisation charge (dual phase) to determine field and energy dependences in liquid argon of both, the light and the charge yields, at working points relevant for dark matter searches.

Acknowledgments

This work is supported by grants from the Swiss National Science Foundation and the Aspera funded DARWIN project.

References

[1] Aprile E *et al.*, 2011 arXiv:1104.2549v3 [astro-ph.CO]
[2] Aprile E *et al.*, 2011 arXiv:1107.2155v1 [astro-ph.IM]
[3] Regenfus C, 2010, DOI: http://dx.doi.org/10.3204/DESY-PROC-2010-03/regenfus_christian
[4] Baudis L, 2010 arXiv:1012.4764v1 [astro-ph.IM] and http://darwin.physik.uzh.ch/
[5] Plante G *et al.*, 2011 arXiv:1104.2587v1 [nucl-ex] (and references therein)
[6] Manalaysay A, 2010 arXiv:1007.3746v1 [astro-ph.IM] (and references therein)
[7] Brunetti R *et al.*, 2005 *New Astr. Rev.* **49** 265
[8] Gastler D *et al.*, 2011 arXiv:1004.0373v2 [physics.ins-det]
[9] Lindhard J and Scharff M, 1961, *Phys. Rev.* **124** 128
[10] Lindhard J, Scharff M and Schiøtt E, 1963, *Mat. Fys. Medd. Dan. Vid. Selsk.* **33/14** 1
[11] Mei D *et al.*, 2008 *Astropart. Phys.* **30** 12
[12] Kubota S *et al.*, 1978 *Phys. Rev. B* **17** 2762
[13] Aprile E *et al.*, 2006 *Phys. Rev. Lett.* **97** 081302
[14] Manzur A *et al.*, 2010 *Phys. Rev. C* **81** 025808
[15] Hitachi A *et al.*, 1983 *Phys. Rev. B* **27/9** 5279
[16] Boccone V *et al.*, 2009 *JINST* **4** P06001
[17] Walter M, Diploma-Thesis Universität Zürich, 2011,
[18] see: http://www.mesytec.com/datasheets/MPD-4.pdf
[19] Amsler C *et al.*, 2010 *JINST* **5** P11003
[20] Amsler C *et al.*, 2008 *JINST* **3** P02001
[21] Acciarri R *et al.*, 2009 *NIM A* **607** 169
[22] Lippincott W *et al.*, 2008 *Phys. Rev. C* **78** 035801 and 2010 *Phys. Rev. C* **81** 039901(E)
[23] Hitachi A *et al.*, 1992 *Phys. Rev. B* **46** 11463
[24] Boccone V, Dissertation Universität Zürich, 2010 *CERN-THESIS*-2010-090
[25] http://www.srim.org, http://physics.nist.gov/PhysRefData/Star/Text/ASTAR.html , ... /ESTAR.html